

See discussions, stats, and author profiles for this publication at: <https://www.researchgate.net/publication/222096568>

# Molecular Dynamics Study of $\epsilon$ -Caprolactone Intercalated in Wyoming Sodium Montmorillonite

ARTICLE *in* LANGMUIR · SEPTEMBER 2003

Impact Factor: 4.46 · DOI: 10.1021/la034491n

---

CITATIONS

24

---

READS

25

6 AUTHORS, INCLUDING:



**Anouk Gaudel Siri**

Aix-Marseille Université

31 PUBLICATIONS 329 CITATIONS

SEE PROFILE



**Fabrice Gardebien**

Université des Antilles et de la Guyane

21 PUBLICATIONS 351 CITATIONS

SEE PROFILE



**Roberto Lazzaroni**

Université de Mons

400 PUBLICATIONS 9,348 CITATIONS

SEE PROFILE

# Molecular Dynamics Study of $\epsilon$ -Caprolactone Intercalated in Wyoming Sodium Montmorillonite

Anouk Gaudel-Siri,<sup>†,‡</sup> Patrick Brocorens,<sup>†</sup> Didier Siri,<sup>§</sup> Fabrice Gardebien,<sup>†</sup>  
Jean-Luc Brédas,<sup>†,||</sup> and Roberto Lazzaroni<sup>\*,†</sup>

*Service de Chimie des Matériaux Nouveaux, Université de Mons-Hainaut, 20 Place du Parc, B-7000 Mons, Belgium, Laboratoire RéSo – UMR 6516, Université d'Aix-Marseille 3, Faculté St. Jérôme, Av. Esc. Normandie-Niemen, 13397 Marseille Cedex 20, France, Laboratoire de Chimie Théorique et Modélisation Moléculaire, CNRS-UMR 6517, Universités d'Aix-Marseille 1 et 3, Faculté St. Jérôme, Av. Esc. Normandie-Niemen, 13397 Marseille Cedex 20, France, and School of Chemistry and Biochemistry, Georgia Institute of Technology, Atlanta, Georgia 30332-0400*

Received March 21, 2003. In Final Form: July 14, 2003

The intercalation process of the  $\epsilon$ -caprolactone monomer into sodium montmorillonite clay is modeled with a combined molecular mechanics/molecular dynamics approach. This study is aimed at understanding the initial stages of caprolactone polymerization within the channels of the clay, to form highly dispersed nanocomposites. The theoretical method is first validated by modeling dry and hydrated Wyoming sodium montmorillonite; the caprolactone-intercalated clay is then investigated, with particular emphasis on the energetics of the intercalation process and the nature of the interactions building up between the organic molecules and the channel walls and sodium counterions.

## 1. Introduction

Poly( $\epsilon$ -caprolactone) (PCL) is a biodegradable aliphatic polyester that is being intensively investigated for use in medical devices and degradable packaging. However, the mechanical properties of the PCL homopolymer are too poor to allow its direct use. To improve the mechanical properties and thermal stability, nanocomposites based on PCL and layered aluminosilicates (montmorillonite-type clay) represent a valuable alternative. Because of the dispersion of nanometer-size clay sheets, nanocomposites exhibit new and improved properties compared to microcomposites or filled polymers.<sup>1,2</sup>

Polymer nanocomposites are usually prepared by melt intercalation; in that procedure, alkali-metal cations of the clay must first be replaced by organic surfactants in order to render the clay channels more organophilic and to allow the intercalation of the polymer. The physicochemical parameters governing the intercalation process and the influence of the organic counterions on the stability of the nanocomposites have been extensively investigated by model calculations (see refs 3–5 and references therein). Those studies allow for the a priori design of composite materials with a well-defined microstructure.

Remarkably, the need for those organophilic counterions can be circumvented if the polymer is directly generated

within the channels. It has been shown recently that the  $\epsilon$ -caprolactone monomers (CL) spontaneously intercalate at ambient temperature between Na-montmorillonite sheets.<sup>6</sup> Subsequent polymerization involving the intercalated monomers then leads to composites with excellent dispersion of the clay sheets in the matrix. To exploit best this new route to polymer nanocomposites, it is essential to obtain a molecular scale description of the intercalation process for the monomer. Through a molecular modeling approach, this study aims at shedding light on (i) the structure of the intercalated system, that is, the spatial distribution of the CL molecules with respect to the clay walls and the counterions, and (ii) the nature of intermolecular interactions favoring intercalation. In turn, this will allow an understanding of whether the spontaneous intercalation of the monomer (and the subsequent polymerization leading to the nanocomposite) is specific to caprolactone, or this new route could be extended to the preparation of other polymer/Na-montmorillonite nanocomposites.

Here we focus on the modeling of the CL-intercalated Na-montmorillonite system. Montmorillonite belongs to the family of 2:1 phyllosilicates. Their crystal structure consists of layers of two silica tetrahedral sheets fused to an edge-shared octahedral sheet of aluminum hydroxide. Stacking of the layers leads to a regular van der Waals gap or interlayer. Isomorphic substitutions within the layers (silicon replaced by aluminum in the tetrahedral sheets and aluminum replaced by magnesium in the octahedral sheet) generate negative charges that are counterbalanced by cations residing in the interlayer region. The natural form of Wyoming montmorillonite contains hydrated Na<sup>+</sup> or K<sup>+</sup> cations. The layer charge of montmorillonite clays is usually between  $-0.5 e$  and  $-1.2 e$  per O<sub>20</sub>(OH)<sub>4</sub> formula unit cell, and octahedral substitutions are responsible for about  $2/3$  of the total charge. We

\* To whom correspondence should be addressed. E-mail: Roberto@averell.umh.ac.be.

<sup>†</sup> Service de Chimie des Matériaux Nouveaux, Université de Mons-Hainaut.

<sup>‡</sup> Laboratoire RéSo – UMR 6516, Université d'Aix-Marseille 3.

<sup>§</sup> Laboratoire de Chimie Théorique et Modélisation Moléculaire, CNRS-UMR 6517, Universités d'Aix-Marseille 1 et 3.

<sup>||</sup> School of Chemistry and Biochemistry, Georgia Institute of Technology.

(1) (a) Krishnamoorti, R.; Vaia, R. A.; Giannelis, E. P. *Chem. Mater.* **1996**, *8*, 1728. (b) Giannelis, E. P. *Adv. Mater.* **1996**, *8*, 29.

(2) Alexandre, M.; Dubois, P. *Mater. Sci. Eng.* **2000**, *R28*, 1.

(3) Vaia, R. A.; Giannelis, E. P. *Macromolecules* **1997**, *30*, 8000.

(4) Giannelis, E. P.; Krishnamoorti, R.; Manias, E. *Adv. Polym. Sci.* **1999**, *138*, 107.

(5) Balazs, A. C.; Singh, C.; Zhulina, E.; Lyatskaya, Y. *Acc. Chem. Res.* **1999**, *32*, 651.

(6) (a) Lepoittevin, B.; Devalckenaere, M.; Pantoustier, N.; Alexandre, M.; Kubies, D.; Calberg, C.; Jérôme, R.; Dubois, P. *Polymer* **2002**, *43*, 4017. (b) Lepoittevin, B.; Devalckenaere, M.; Alexandre, M.; Pantoustier, N.; Calberg, C.; Jérôme, R.; Dubois, P. *Macromolecules* **2002**, *35*, 8385.

**Table 1. Atomic Charges<sup>a</sup>**

	atom								
	C <sub>1</sub>	C <sub>2</sub>	C <sub>3</sub>	C <sub>4</sub>	C <sub>5</sub>	O <sub>6</sub>	C <sub>7</sub>	O <sub>8</sub>	H <sub>9</sub>
charge/e	-0.20	-0.28	-0.28	-0.24	0.00	-0.52	0.64	-0.47	0.13

	atom								
	H <sub>10</sub>	H <sub>11</sub>	H <sub>12</sub>	H <sub>13</sub>	H <sub>14</sub>	H <sub>15</sub>	H <sub>16</sub>	H <sub>17</sub>	H <sub>18</sub>
charge/e	0.10	0.16	0.13	0.14	0.14	0.18	0.10	0.14	0.12

	atom						
	Si	Al <sup>b</sup>	Mg	O (OH)	H	O (bridge)	O
charge/e	1.2	3.0 or 0.2	2.0	-1.424	0.424	-1.0	-0.8

<sup>a</sup> For the CL molecule, atomic charges are optimized with the QEq algorithm; for montmorillonite, they are assigned according to the method due to Skipper et al. (ref 7a). <sup>b</sup> The partial charge of the Al atoms is 3.0 in the octahedral sites and 0.2 when they replace a Si atom in the tetrahedral sheet.

here consider the unit cell formula  $\text{Na}_{0.75}(\text{Si}_{7.75}\text{Al}_{0.25})-(\text{Al}_{3.5}\text{Mg}_{0.5})\text{O}_{20}(\text{OH})_4$  which represents a mineral with a charge of  $-0.75 e$ . This particular clay is chosen because of its wide use in the preparation of polymer nanocomposites.

Molecular dynamics (MD) simulations are performed to obtain information on the geometrical aspects of the intercalation process and to collect average data about the interlayer species. As a preliminary step aimed at evaluating the reliability of our approach, dry montmorillonite is simulated and our results for this system are compared to previous theoretical and experimental studies.<sup>7</sup> We then proceed to the simulation of the CL-intercalated system; the results are analyzed in terms of the orientation of the CL molecules in the interlayer channel, their interaction with the  $\text{Na}^+$  cations, and the energetics of the intercalated system.

## 2. Computational Methodology

For this study, we used the molecular dynamics module and the energy minimizer of the Cerius<sup>2</sup> 4.0 package.<sup>8</sup> Due to the presence of organic and inorganic species, the universal force field (UFF)<sup>9</sup> was selected.

**2.1. Caprolactone Molecule.** The geometry of the isolated CL molecule was optimized with the UFF. During the energy minimization, the partial charges of the atoms were optimized with the QEq algorithm;<sup>10</sup> they are reported in Table 1. As found in previous experimental and theoretical studies,<sup>11</sup> the seven-membered ring of CL preferentially adopts a chair conformation (Figure 1).

**2.2. Dry Na-Montmorillonite.** The simulation system consists of a periodically replicated, rectangular box that contains eight Na-montmorillonite unit cells ( $4 \times 2 \times 1$ ). The dimensions of the starting box are  $a = 20.8 \text{ \AA}$ ,  $b = 18.4 \text{ \AA}$ , and  $c = 12.0 \text{ \AA}$ . The starting system is monoclinic

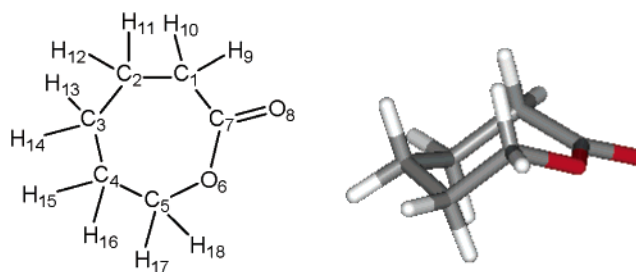


**Figure 1.** Atom numbering and chair conformation of the CL molecule.

with  $\beta = 99^\circ$ , as in the unit cell of dry montmorillonite.<sup>12</sup> The positions and charges of the sites in the unit cell of the clay are directly derived from the empirical model introduced by Skipper et al.<sup>7a</sup> (Table 1): four isomorphous substitutions of trivalent Al atoms by divalent Mg atoms in the octahedral sheet and two isomorphous substitutions of tetravalent Si atoms by trivalent Al atoms in the tetrahedral sheets. Six  $\text{Na}^+$  counterions are placed in the interlayer region.

**2.3. Na-Montmorillonite with Intercalated CL Molecules.** In a preliminary MD study of hydrated Na-montmorillonite with the UFF, we have found that the density of water in the interlayer region (0.95) is very close to the density of liquid water. On that basis, we assume that the density of CL between the clay sheets is close to the density of liquid CL (1.03). Moreover, X-ray diffraction data<sup>6a</sup> provide the  $d_{001}$  parameter of Na-montmorillonite with intercalated CL molecules (19.6  $\text{\AA}$ ). If we subtract the volume of the simulation cell of dry Na-montmorillonite at equilibrium (3735  $\text{\AA}^3$ ) from the calculated volume of a monoclinic Na-montmorillonite with  $d_{001} = 19.6 \text{ \AA}$  (7410  $\text{\AA}^3$ ), we obtain a volume of 3675  $\text{\AA}^3$  occupied by CL molecules. With a density of 1.03, this corresponds to about 18 CL molecules in the simulation cell. Therefore, for the simulation of the CL-intercalated system, the starting point is the monoclinic system of dry Na-montmorillonite, with the  $c$  parameter enlarged to 20.0  $\text{\AA}$  and 18 CL monomer molecules inserted in the interlayer spacing. Let us recall that since the polymerization of caprolactone is most efficient when the medium is anhydrous, the clay is usually dried before the monomer incorporation.<sup>6</sup> Therefore, water-free montmorillonite appears to be the most suitable system to model CL intercalation.

**2.4. Molecular Dynamics Simulations.** For the two periodic systems (dry and CL-intercalated Na-montmorillonite), the configuration of the starting simulation cell is replicated in all three spatial directions through periodic boundary conditions. Ewald summation methods<sup>13</sup> are used to treat Coulombic and attractive van der Waals interactions with a standard cutoff. Repulsive van der Waals interactions are directly calculated with standard parameters. All simulations are performed at a constant temperature using a "weak coupling" algorithm<sup>14</sup> and a coupling time constant of 500 fs. The Verlet algorithm and a time step of 1 fs are used for all dynamics simulations.

To reduce the computational effort, we impose that the atoms in the clay sheets remain at constant positions during the MD calculation, as the sheets are expected to

(7) (a) Skipper, N. T.; Refson, K.; McConnell, J. D. C. *J. Chem. Phys.* **1991**, *94*, 7434. (b) Karaborni, S.; Smit, B.; Heidug, W.; Urai, J.; Oort, E. v. *Science* **1996**, *271*, 1102. (c) Young, D. A.; Smith, D. E. *J. Phys. Chem. B* **2000**, *104*, 9163. (d) Park, S.-H.; Sposito, G. *J. Phys. Chem. B* **2000**, *104*, 4642. (e) Chavez-Paez, M.; Van Workum, K.; de Pablo, L.; de Pablo, J. J. *J. Chem. Phys.* **2001**, *114*, 1405.

(8) Molecular Simulations Inc., 9685 Scranton Road, San Diego, CA; 1997.

(9) (a) Rappé, A. K.; Casewit, C. J.; Colwell, K. S.; Goddard, W. A., III; Skiff, W. M. *J. Am. Chem. Soc.* **1992**, *114*, 10024. (b) Casewit, C. J.; Colwell, K. S.; Rappé, A. K. *J. Am. Chem. Soc.* **1992**, *114*, 10035. (c) Casewit, C. J.; Colwell, K. S.; Rappé, A. K. *J. Am. Chem. Soc.* **1992**, *114*, 10046.

(10) Rappé, A. K.; Goddard, W. A., III *J. Phys. Chem.* **1991**, *95*, 3358.

(11) (a) Abraham, R. J.; Gherzi, A.; Petrillo, G.; Sancassan, F. *J. Chem. Soc., Perkin Trans. 2* **1997**, 1279. (b) Allen, F. H.; Howard, J. A. K.; Pitchford, N. A.; Vinter, J. G. *Acta Crystallogr., Sect. B* **1994**, *382*.

(12) Brindley, G. W.; Brown, G. *Crystal Structures of Clay Minerals and Their X-ray Identification*; Mineralogical Society: London, 1980.

(13) Karasawa, N.; Goddard, W. A., III *J. Phys. Chem.* **1989**, *93*, 7320.

(14) Berendsen, H. J. C.; Postma, J. P. M.; van Gunsteren, W. F.; DiNola, A.; Haak, J. R. *J. Chem. Phys.* **1984**, *81*, 3684.



be fully rigid. However, as a consequence, *NPT* dynamics simulations (i.e., performed at constant number of particles, pressure, and temperature) are not possible (since the volume would be allowed to change) and we have to carry out successive, alternating *NVT* dynamics simulations and energy minimization steps, also using the UFF. During *NVT* dynamics simulations, the clay sheets are immovable, but when energy minimizations are performed, registry and swelling motions are allowed. The “smart minimizer” of the Cerius<sup>2</sup> package is used with 2500–5000 iterations. The RMS-force criterion is 0.005 kcal mol<sup>-1</sup> Å<sup>-1</sup>, the criterion on the energy difference is 10<sup>-5</sup> kcal mol<sup>-1</sup>, and the criterion on the RMS-shift is  $3 \times 10^{-5}$  Å.

For the clay with intercalated CL molecules, a procedure in three steps is followed:

(1) The initial optimization of the cell parameter *c* leads to a value of 19.4 Å. Then, the cell parameters are frozen and short *NVT* dynamics simulations (20 ps) are performed at increasing temperatures from 300 to 600 K in increments of 50 K. This first step allows the system to overcome potential barriers and rearrange itself into a state with improved interactions among CL molecules, between Na<sup>+</sup> cations and CL molecules, and between the clay sheets and CL molecules at a starting cell parameter *c* of 19.4 Å.

(2) *NVT* dynamics simulations (20 ps) at 300 K alternate with energy minimizations in order to optimize the interlayer spacing. At first, the cell parameter *c* is the only degree of freedom. As soon as *c* is optimized in the monoclinic space group (*c* = 18.3 Å), registry motions are allowed: two degrees of freedom ( $\alpha$  and  $\beta$ ) are added. Therefore, the three parameters  $\alpha$ ,  $\beta$ , and *c* are simultaneously optimized and the equilibrium configuration is obtained. This step-by-step strategy prevents the system from evolving toward irrelevant and less stable configurations with a large sliding of the two clay sheets.

(3) We start from the equilibrium configuration found in step 2, and a *NVT* dynamics simulation of 460 ps is performed at 300 K. We observe that the system reaches equilibration after 50 ps; then average data are collected over 410 ps.

For dry Na-montmorillonite, steps 1 and 2 lead to the equilibrium configuration.

### 3. Results and Discussion

**3.1. Dry Na-Montmorillonite.** From this dynamics study with the UFF, we obtain  $d_{001} = 9.88$  Å,  $\alpha = 97^\circ$ , and  $\beta = 95^\circ$  for the equilibrium configuration (Figure 2). These results are very close to experimental data ( $9.55 < d_{001} < 9.8 \pm 0.1$  Å,  $\alpha = 90^\circ$ , and  $\beta = 99^\circ$ ) and previous MD and Monte Carlo calculations ( $9.7 < d_{001} < 9.8$  Å).<sup>7</sup> This clearly demonstrates the validity of our theoretical approach. We only note a slight registry motion of the clay sheets since  $\alpha$  and  $\beta$  differ from the starting values. In agreement with previous studies, the equilibrium position of Na<sup>+</sup> cations is in the hexagonal sites, where the cation is nestled within two hexagonal cavities of opposite tetrahedral sheets (Figure 2b). Most of the Na<sup>+</sup> cations are 6 Å apart, but two of them, which are close to the isomorphic substitution of a Si atom, are only 5.0 Å apart (Figure 2b). From the analysis of the different energy terms, it appears that the stability of the clay is mainly due to electrostatic interactions.

**3.2. Na-Montmorillonite with Intercalated CL Molecules.** As a preliminary step to investigate the orientational behavior of the molecules, we placed 6 CL molecules in the interlayer spacing with different starting

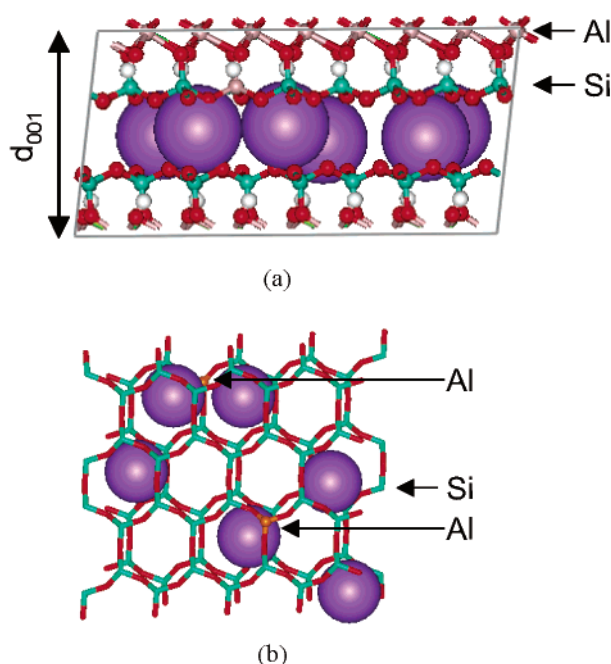


**Figure 2.** Equilibrium configuration of dry Na-montmorillonite. Only the Na<sup>+</sup> cations are shown with their van der Waals radius. (a) Side view with the atoms of the clay sheets in a “ball and stick” representation. (b) Top view. Only the SiO<sub>3</sub> moieties (sticks) of the tetrahedral sheets surrounding the Na<sup>+</sup> cations are shown.

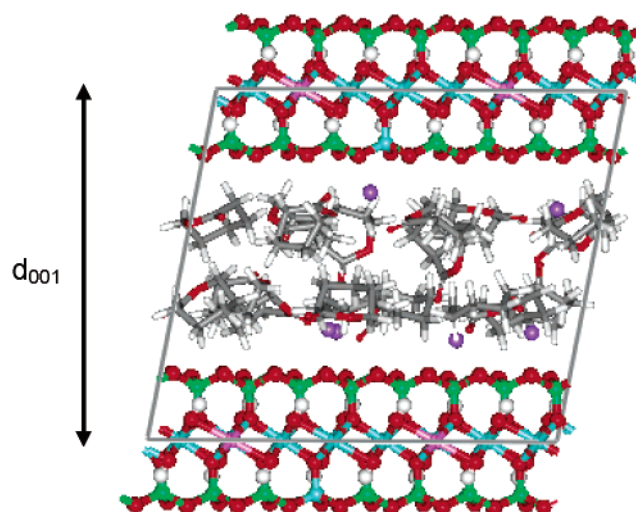


**Figure 3.** Equilibrium configuration of Na-montmorillonite intercalated with CL molecules.

orientations relative to the clay sheets. Short MD simulations led to a similar orientation, with the CL rings preferentially oriented to maximize their interaction with the clay sheets, that is, the chair is roughly parallel to the surface of the sheet. Therefore, when considering the “fully loaded” system, the 18 CL molecules form two layers, roughly parallel to the channel walls. The Na<sup>+</sup> counterions are distributed between the CL layers and the clay sheets. During MD simulations, the geometry of the CL rings is allowed to change but the partial charges are fixed.

From these calculations, we obtain  $d_{001} = 18.17$  Å,  $\alpha = 87.6^\circ$ , and  $\beta = 100.8^\circ$  for the equilibrium configuration (Figure 3). We find a slight registry motion of the clay sheets for this system as well. The volume of the box is 6824 Å<sup>3</sup>, implying that the remaining volume for CL molecules is 3090 Å<sup>3</sup>. This corresponds to a density of 1.10 for the interlayer phase (close to the density of liquid CL).

The average intercalation energy of a CL molecule in the interlayer spacing of dry Na-montmorillonite is defined as

$$\Delta U = [U(18) - U(0) - 18U(\text{CL})]/18$$

$U(18)$  and  $U(0)$  are the equilibrium configuration potential energies of intercalated and dry Na-montmorillonite, respectively; and  $U(\text{CL})$  is the potential energy of one CL molecule. We find a large negative value for  $\Delta U$  ( $-35.9$  kcal mol $^{-1}$ ). We have to subtract from that value the solvation energy of CL, which is included in  $U(18)$  but not in  $U(\text{CL})$ ; from a calculation on a cluster of 18 CL molecules, it is estimated to be around 20 kcal mol $^{-1}$ . Therefore, the global stabilization upon intercalation is around 16 kcal mol $^{-1}$  per molecule, which indicates that from the energetic point of view, the spontaneous intercalation of CL molecules in Na-montmorillonite is highly favorable. The entropy balance of the intercalation process cannot be estimated from our calculations. However, for a similar system (polystyrene intercalated in montmorillonite channels), Vaia and Giannelis<sup>3,4</sup> have performed detailed mean-field studies to evaluate the energetic and entropic aspects of the intercalation process. They have shown that the loss of conformational freedom of the molecules upon intercalation can be compensated by the entropic gain of the ions present in the cavity, due to the increase in the clay sheet separation. In particular, this compensation is complete (i.e., the entropic balance is neutral) when the gallery height increases by less than 1 nm, as is the case in our systems. Those results have been obtained for alkylammonium counterions; the same compensating effect must be at work in the Na-containing compounds studied here, even though to a significantly smaller extent (because the Na $^{+}$  cations tend to remain close to the channel walls, see below). Nevertheless, the entropic balance is expected not to be strongly unfavorable in our systems. This, combined with a clear energetic stabilization, is consistent with the observation of spontaneous intercalation.

To gain information on (i) the spatial distribution of the various species within the channels and (ii) the nature of the interactions among those species, average positional data are collected during the late stages of the MD simulations, after the system has reached equilibration. Radial distribution functions are calculated between Na $^{+}$  cations and the oxygen atoms of CL molecules in order to estimate the solvation of Na $^{+}$  cations by CL molecules; the interaction between Na $^{+}$  cations and the oxygen atoms of the clay is evaluated as well. Radial distribution functions are defined as follows:

$$g_{AB}(r) = \frac{dn_r}{4\pi\rho_B r^2 dr}$$

where  $dn_r$  is the number of B particles in a shell between  $r$  and  $r + dr$  around each A particle and  $\rho_B$  is the density of B particles. The number of nearest neighbors is deduced from the radial distribution function:

$$N_{AB} = 4\pi\rho_B \int_0^{\text{cutoff}} g_{AB}(r)r^2 dr$$

where the cutoff is defined in order to consider only the first peak of the radial distribution function. The results are reported in Figure 4.

On average, the first solvation shell of Na $^{+}$  cations is composed of 3 carbonyl oxygen atoms ( $d(\text{Na}-\text{O}) = 2.29$  Å) and 1.6 intracyclic oxygen ( $d(\text{Na}-\text{O}) = 2.25$  Å) from CL

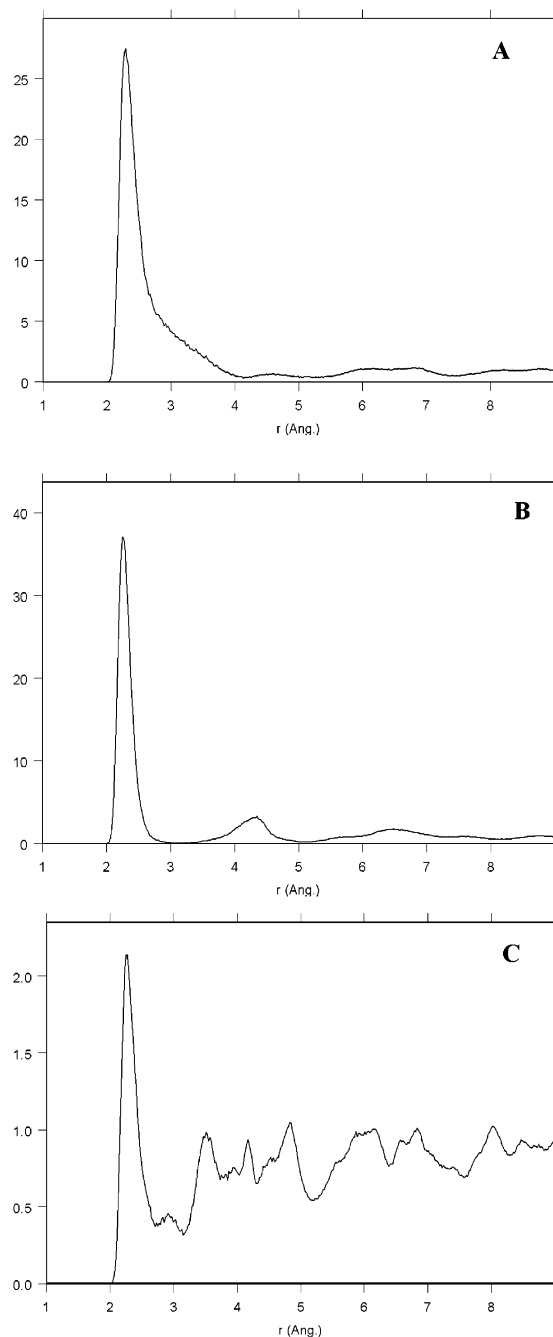


**Figure 4.** Radial distribution functions around Na $^{+}$  cations for (A) the carbonyl oxygen atoms of CL, (B) the intracyclic oxygen atoms of CL, and (C) the clay oxygen atoms.

molecules and 2 oxygen atoms from the silicate sheets ( $d(\text{Na}-\text{O}) = 2.27$  Å). In terms of coordination number, these results are quite similar to those of recent calculations<sup>15</sup> dealing with the hydration of Na $^{+}$  cations (5 or 6 water molecules in the first solvation shell). The ability of CL molecules to solvate the Na $^{+}$  cations in the interlayer spacing is therefore likely an important factor contributing to the spontaneous intercalation process.

Density profiles of the interlayer species are determined through calculations of their probability distribution

(15) (a) Degève, L.; Quintale, C., Jr. *J. Chem. Phys.* **1994**, *101*, 2319. (b) Obst, S.; Bradaczek, H. *J. Phys. Chem.* **1996**, *100*, 15677. (c) Lee, S. H.; Rasaiah, J. C. *J. Phys. Chem.* **1996**, *100*, 1420. (d) Koneshan, S.; Rasaiah, J. C.; Lynden-Bell, R. M.; Lee, S. H. *J. Phys. Chem. B* **1998**, *102*, 4193. (e) White, J. A.; Schwegler, E.; Galli, G.; Gygi, F. *J. Chem. Phys.* **2000**, *113*, 4668.

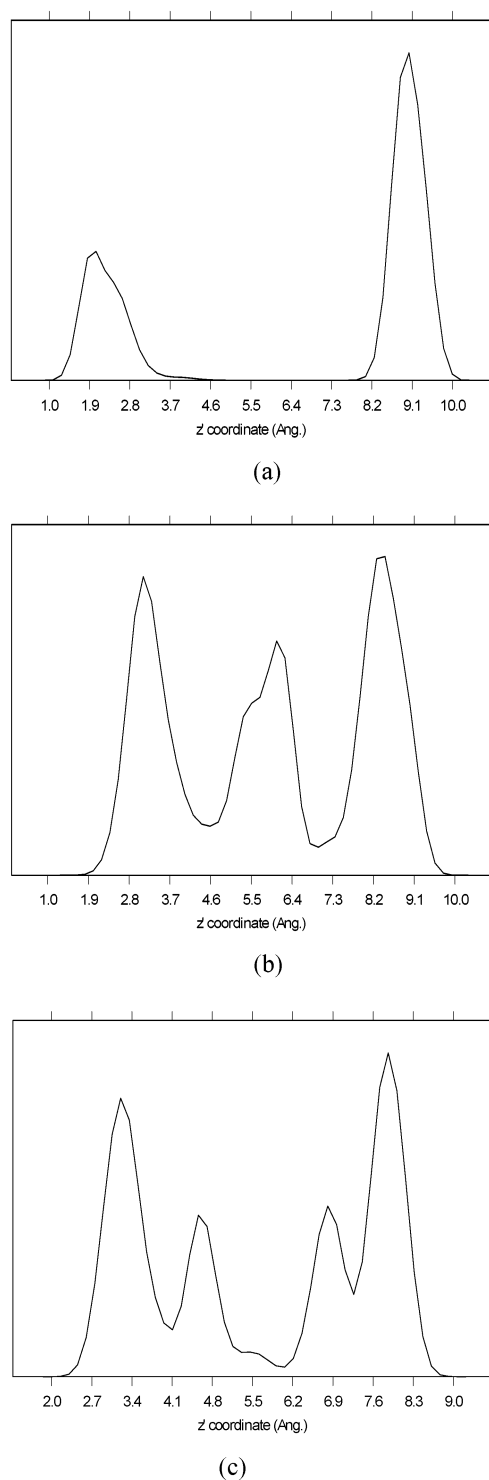


**Figure 5.** Density profiles for (a) the Na<sup>+</sup> cations, (b) the carbonyl oxygen atoms of CL, and (c) the intracyclic oxygen atoms of CL. The *z*-coordinate corresponds to the direction perpendicular to the clay sheets.

functions in the *z* direction, that is, the direction perpendicular to the plane of the clay sheet (Figure 5). Na<sup>+</sup> cations are distributed close to the clay sheets, while the

CL molecules form two layers with various orientations of the carbonyl and intracyclic oxygen atoms. The distribution of the Na<sup>+</sup> cations is not symmetric: four cations are close to the first clay sheet while only two are close to the second sheet (Figure 5a). Most of the oxygen atoms are oriented toward Na<sup>+</sup> cations and contribute to their solvation. This partial solvation of the Na<sup>+</sup> cations (which are still in interaction with the clay sheets) is a driving force that is consistent with the spontaneous intercalation of CL molecules in Na-montmorillonite. Some carbonyl oxygen atoms are located in the middle of the interlayer spacing and are surrounded by two sheets of intracyclic oxygen atoms (Figure 5b,c). This corresponds to groups that do not participate in the solvation of Na<sup>+</sup> cations. As a result, the spatial distribution of the oxygen atoms (and consequently that of the CL molecules) is symmetric with respect to the cavity wall (Figure 5b,c), despite the asymmetry in the distribution of the cations.

#### 4. Concluding Remarks

The results of our MD study provide insight into the structure and energetics of Wyoming Na-montmorillonite intercalated with caprolactone monomers. The interaction between the clay sheets of Na-montmorillonite and CL molecules and the partial solvation of the Na<sup>+</sup> cations by CL molecules are two energetic factors that favor the spontaneous intercalation of the monomers. These two factors are also at work to some extent for intercalated PCL. However, with respect to the monomer, the incorporation of the solvating groups in polymer chains is expected to decrease the efficiency of solvation and the strength of the interaction with the walls, especially in confined spaces such as clay channels. In addition, the loss of configurational freedom that the polymer chains undergo when intercalating raises the entropic price to be paid for their intercalation to a much higher level than for the CL molecules.<sup>3–5</sup> Therefore, it appears that the enthalpic factor overcomes the entropic factor only for the monomer, since spontaneous intercalation is observed for the monomer and not for the polymer.<sup>6,16</sup> More generally, we believe that the modeling approach followed in this work could be applied to investigate the structural and energetic aspects of the intercalation of other monomers in Na-montmorillonite, to determine a priori the feasibility of the in situ polymerization route. Clearly, this work indicates that favorable interactions with the channel walls and solvation of the Na<sup>+</sup> cations are prerequisites for efficient monomer intercalation.

**Acknowledgment.** The authors are grateful to Ph. Dubois, M. Alexandre, and E. Pollet (Université de Mons-Hainaut) for many fruitful discussions. This project is supported by the Government of the Région Wallonne, in the framework of the WDU program (TECMAVER). Research in Mons is also partly supported by the Belgian Federal Government (IAP Project V/3) and the Belgian National Fund for Scientific Research FNRS/FRFC. R.L. is "Directeur de Recherches du Fonds National de la Recherche Scientifique" (FNRS – Belgium).

LA034491N

(16) LeBaron, P. C.; Wang, Z.; Pinnavaia, T. J. *Appl. Clay Sci.* **1999**, *15*, 11.